Shock and Vibration 18 (2011) 317–331
DOI 10.3233/SAV-2010-0569
IOS Press

Lateral vibration of hydroelectric generating set with different supporting condition of thrust pad

Xiaohui Si, Wenxiu Lu and Fulei Chu*
Department of Precision Instruments and Mechanology, Tsinghua University, Beijing, P.R. China

Received 7 February 2010
Revised 25 April 2010

Abstract. The variations of the supporting condition, which change the stiffness of tilting pad thrust bearing, may alter the dynamic behavior of the rotor system. The effects of supporting condition of thrust pad on the lateral vibration of a hydroelectric generating set are investigated in this paper. The action of a thrust bearing is described as moments acting on the thrust collar, and the tilting stiffness coefficients of thrust bearing are calculated. A model based on typical beam finite element method is established to calculate the dynamic response, and the effects of supporting conditions such as elastic oil tank support, different heights of the thrust pads with rigid support are discussed. The results reveal that the influence of thrust bearing is small when the elastic oil tanks work normally. When the supporting conditions turn to be rigid due to the oil leakage, the differences of thrust pad heights have evident influence on the load distribution of the thrust pads; while the effects on the tilting stiffness of the thrust bearing and the amplitude of the lateral shaft vibration is small when the maximum load on thrust pads is smaller than the allowable value.

Keywords: Rotor dynamics, thrust bearing, lateral vibration, tilting stiffness

1. Introduction

In many industrial applications, rotating machinery such as hydroelectric generating set supported by journal bearings are also equipped with a thrust bearing in order to prevent the axial movement and balance the axial force. The dynamic behavior of the shaft strongly depends on these bearings whose influences are often introduced in rotordynamics with dynamic coefficients.

There has been much research focusing on the influences of journal bearings on the dynamic behavior of the rotor system. However, the effects on the lateral shaft vibration of hydrodynamic thrust bearing have not been investigated so extensively as those of journal bearings. The dynamic coefficients of hydrodynamic thrust bearing and the effects on axial vibration were presented by Someya and Fukuda [1], Storteig and White [2], and Zhu et al. [3], and the identification of a hydrodynamic thrust bearing is discussed in reference [4,5]. Mittwollen et al. [6] studied the effects of hydrodynamic thrust bearing on the lateral vibration of a rotor system. They defined a series of dynamic coefficients to describe the dynamic action of a hydrodynamic thrust bearing, and the effects of a thrust bearing on the lateral vibration of a single-mass rotor system were investigated theoretically and experimentally. Yu et al. [7–9] provided extensive and systemic research into the behavior of a rotor-bearing system equipped with a hydrodynamic thrust bearing. Berger et al. [10] presented the coupling between axial vibration and bending vibration of a flexible shaft due to the thrust bearing.

*Corresponding author. Tel.: +86 10 62792842; Fax: +86 10 62792842; E-mail: chufl@mail.tsinghua.edu.cn.

ISSN 1070-9622/11/$27.50

Previous research on thrust bearing was focused on the dynamic coefficients of the oil film of fixed pad. However, thrust bearings with tilting pad are commonly used when the axial load is large. Though the dynamic behavior of oil film is similar to that of fixed pad, the supporting conditions cannot be treated as rigid, especially when the thrust pad is supported by elastic oil tank with considerable deformation in the operation of the hydroelectric generating set. Therefore, the stiffness of supporting condition affects the tilting stiffness of the thrust bearing and the dynamic behavior of the lateral shaft vibration. When faults occur, such as oil leakage in the elastic oil tank, the supporting condition will be changed, and both the tilting stiffness of the thrust bearing and the distribution of loads on the thrust pads will be changed. Moreover, the aim of the most previous research was to investigate the relationship between the effect of thrust bearing and the continuous variation of parameters, where those parameters may be beyond some restraints. For instance, the film thickness of thrust pad might be smaller than the allowable minimum, or the load on thrust pad may exceed the allowable value, which are impermissible in the practical process of machines.

In this paper, the tilting stiffness coefficients of the thrust bearing are calculated under different supporting conditions of the thrust pads, especially when oil leakage occurs at the elastic oil tank. The amplitude of the lateral shaft vibration and the load distribution of the thrust pads are also investigated theoretically based on the tilting stiffness.

Hydroelectric generating set is a complex system, the vibration of which could be caused by many excitations, while only mechanical and electromagnetic ones are considered in this paper. More excitations will make the result closer to the real condition. The vibration is influenced obviously by the boundary conditions and system parameters, such as stiffness and damping of bearings, including guide bearing and thrust bearing, which have obvious nonlinear characteristics, while only main boundary conditions with linear model are introduced and the damping of thrust bearing is ignored in this paper for the sack of convenience. Therefore, more accurate results will be obtained when more boundary conditions with nonlinear model are adopted. In addition, the influence of the thrust bearing on the lateral shaft vibration can be affected by many factors, such as axial load, stiffness of the shaft, static load on the guide bearings, position and arrangement of the thrust bearing et al. [9], while all the parameters mentioned in this paper are selected according to a real set in Fujian province in China. Therefore, the results obtained are reasonable for the certain parameters, while the method proposed in this paper is general for the analysis of the influence of the thrust bearing on the lateral vibration of hydroelectric generating set.

2. Configuration of hydroelectric generating set and elastic oil tank

2.1. Hydroelectric generating set

The shaft system of hydroelectric generating set, as shown in Fig. 1, mainly consists of the following components: upper guide bearing (UGB), generator rotor, thrust bearing, flange, water guide bearing (WGB) and turbine runner. The UGB and WGB provide the constraint in lateral direction, and the thrust bearing bears the axial load including gravity of the shaft system and water thrust acting on the turbine runner. For the safe operation of the hydroelectric generating set, both the amplitude of the lateral shaft vibration and the load on the thrust pad should not exceed the allowable values.

2.2. Elastic oil tank

The design of a thrust pad supported by elastic oil tank is shown in Fig. 2. The main support parts in the elastic oil tank are top cover, corrugated tube and pillar support, and the oil in different oil tanks is connected via the oil way in the chassis. When the elastic oil tank works normally, the width of clearance between the top cover and pillar support is always kept in 2–3 mm, and the most loads are supported by the oil pressure. After a longtime operation, oil leakage may occur which increases the axial deformation of the corrugated tube, and the supporting condition will approach rigid when the top cover touches the pillar support finally. In this condition, the distance from the upper surface of the thrust pad to the upper surface of the chassis is defined as Thrust Pad Height (Fig. 2).

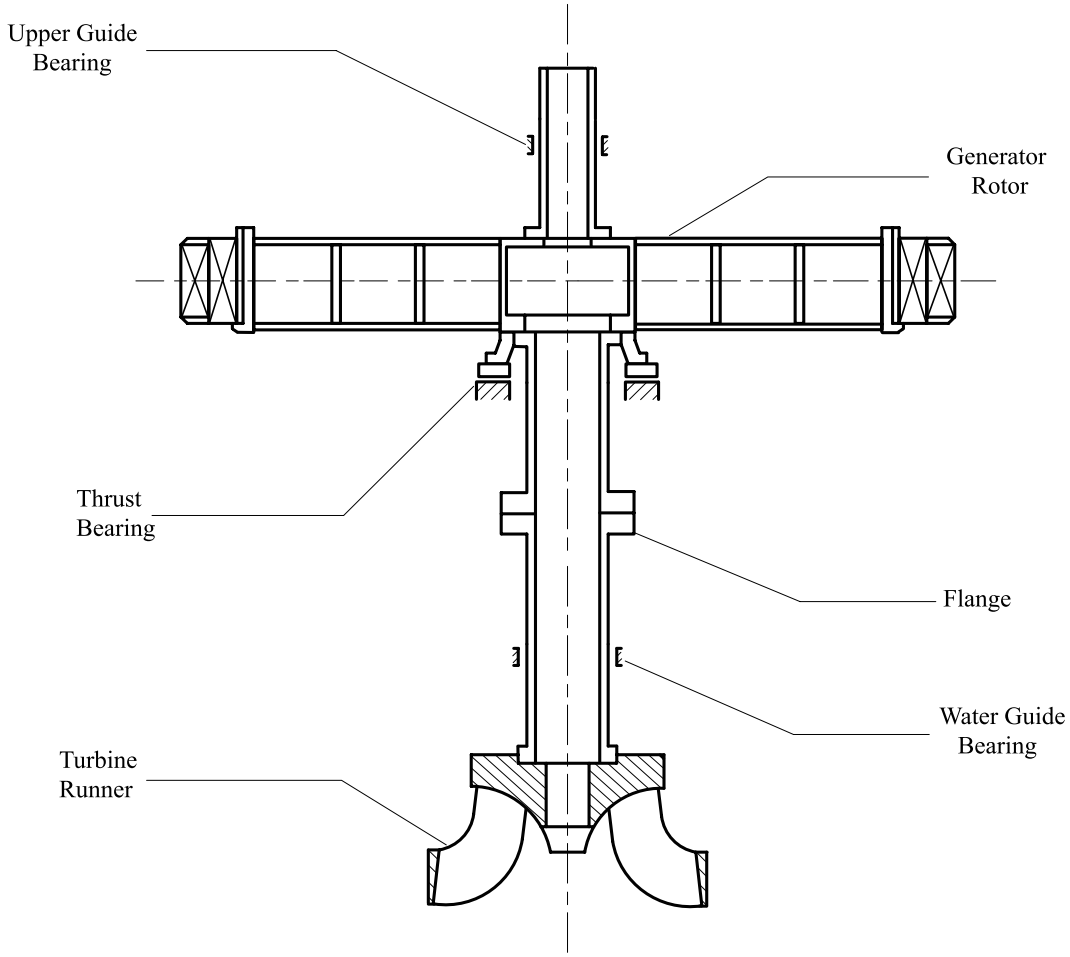

Fig. 1. Schematic diagram of the shaft system of hydroelectric generating set.

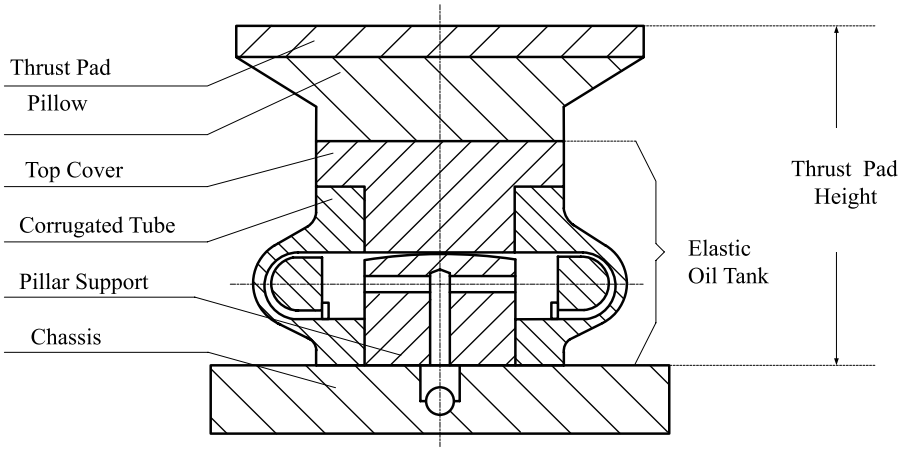

Fig. 2. Schematic diagram of support components of thrust pad.

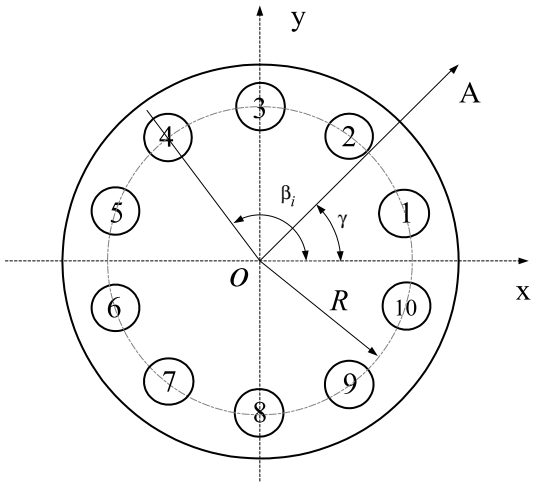

Fig. 3. Configuration of thrust pad distribution.

3. Formulations

3.1. Thrust bearing model

A change of the tilting angle of thrust collar changes the axial displacement of thrust pads and therefore alters the moment acting on the thrust collar due to the stiffness and damping. Extensive investigations have been focused on the static and dynamic coefficients of thrust bearing and relative calculation could be found in many literatures, and only the essential modifications and derivation are presented in this section.

The thrust bearing is assumed to work in the isothermal condition. The pressure distribution of oil film between the thrust collar and thrust pad is calculated from the *Reynolds Equation* by using finite difference method. The oil film force F_{oil} is calculated by integrating the pressure p on the surface of thrust pad s.

$$F_{oil} = \iint_s pds \tag{1}$$

And the vertical stiffness of the oil film is calculated by

$$K_{oil} = \frac{dF_{oil}}{dh_p} \tag{2}$$

where h_p represents the film thickness at the fulcrum.

Among the supporting parts, the deformation of the elastic oil tank cannot be ignored, and its axial stiffness is represented as K_{tank} which could be obtained by numerical simulation using *ANSYS*. Because the oil film and the oil tank bear the load in series, when the chassis is assumed as horizontal and the elastic deformations of the other supporting components are ignored, the equivalent axial stiffness of a single pad can be obtained as

$$K_v = \frac{K_{oil} \times K_{tank}}{K_{oil} + K_{tank}} \tag{3}$$

For the lateral shaft vibration, the influence of the thrust bearing on the shaft is in the form of moment. The oil has no effect on the moment when the gravity is ignored because the oil in all tanks is connected. Therefore, K_{tank} can be calculated with the case that there is no oil in the tank. However, if the investigation is focused on the axial behavior of the shaft, the influence of oil pressure should be taken into account. In the following analysis, when the top cover touches the pillar support, K_{tank} is set to be infinite since the contact stiffness is far larger than the oil film stiffness.

The distribution of the thrust pads is shown in Fig. 3. For the ith thrust pad, when the thrust collar has a small tilting angle θ in the direction of OA, the amplitude of the reaction and the arm of force can be represented as

$$K_{vi}R\theta\left|\sin\left(\beta_i-\gamma\right)\right|$$

$$R\left|\sin\left(\beta_i-\gamma\right)\right|$$

where K_{vi} is the equivalent axial stiffness of ith oil tank, i the number of tank (Fig. 3), and R the radius of the circle where the oil tanks are fixed. The total reaction moment in the direction of OA acting on the thrust collar can be represented as

$$R^2\theta\sum_{i=1}^{n}K_{vi}\sin^2\left(\beta_i-\gamma\right) \tag{4}$$

where n is the total number of thrust pads. And the total reaction moment in vertical direction of OA is zero. Thus, the tilting stiffness of thrust bearing in the direction of OA can be written as

$$R^2\sum_{i=1}^{n}K_{vi}\sin^2\left(\beta_i-\gamma\right) \tag{5}$$

When the elastic oil tanks work normally, the loads on all the pads are identical because of the connecting oil. Therefore, all the thrust pads have the same equivalent axial stiffness

$$K_{vi}=K_v, i=1,2,3\cdots n$$

Thus, the tilting stiffness of the thrust bearing can be represented as

$$K_vR^2\sum_{i=1}^{n}\sin^2\left(\beta_i-\gamma\right)$$

Therefore, the tilting stiffness in the coordinate system shown in Fig. 3 can be written as

$$K_{xx}=K_vR^2\sum_{i=1}^{n}\sin^2\left(\beta_i\right),\ K_{yy}=K_vR^2\sum_{i=1}^{n}\sin^2\left(\beta_i-\frac{\pi}{2}\right) \tag{6}$$

There is no coupling in two directions, and it is easy to find that the two stiffness coefficients are equal.

When the contact between the top cover and the pillar support occurs, the load on each of them could be considered as equal if all the thrust pads have the same height, and the stiffness coefficients have the same form as in Eq. (6). Nevertheless, due to the error in manufacturing and installation, the height differences between the thrust pads are unavoidable. Then, the tilting in x and y directions may be coupled.

When the tilting angle is θ_y, as shown in Eq. (4), the reaction moment acting on the thrust collar in y direction can be represented as

$$M_{yy}=R^2\theta_y\sum_{i=1}^{n}K_{vi}\sin^2\left(\beta_i-\pi/2\right)$$

For ith tank, the reaction moment in x direction can be presented as

$$M_{xyi}=\begin{cases}-K_{vi}R\theta_y\left|\sin\left(\beta_i\right)\right|R\left|\cos\left(\beta_i\right)\right|, & 0\leqslant\beta_i\leqslant\pi/2\\ K_{vi}R\theta_y\left|\sin\left(\beta_i\right)\right|R\left|\cos\left(\beta_i\right)\right|, & \pi/2<\beta_i\leqslant\pi\\ -K_{vi}R\theta_y\left|\sin\left(\beta_i\right)\right|R\left|\cos\left(\beta_i\right)\right|, & \pi<\beta_i\leqslant3\pi/2\\ K_{vi}R\theta_y\left|\sin\left(\beta_i\right)\right|R\left|\cos\left(\beta_i\right)\right|, & 3\pi/2\leqslant\beta_i\leqslant2\pi\end{cases} \tag{7}$$

According to the sign of function value of β_i, Eq. (7) could be simplified as

$$M_{xyi}=-K_{vi}R^2\theta_y\sin\left(\beta_i\right)\cos\left(\beta_i\right)$$

In this way, the total reaction moment in x direction acting on the thrust collar can be arranged as

$$M_{xy}=\sum_{i=1}^{n}M_{xyi}=-R^2\theta_y\sum_{i=1}^{n}K_{vi}\sin\left(\beta_i\right)\cos\left(\beta_i\right)$$

Using the same method, when the tilting angle is θ_x the reaction moment of the thrust bearing in x and y directions are

$$M_{xx} = R^2\theta_x \sum_{i=1}^{n} K_{vi} \sin^2(\beta_i), M_{yx} = R^2\theta_x \sum_{i=1}^{n} K_{vi} \sin(\beta_i)\cos(\beta_i)$$

The reaction moment exerted on the thrust collar caused by the tilting angle can be represented as

$$\begin{Bmatrix} M_x \\ M_y \end{Bmatrix} = \begin{Bmatrix} M_{xx} + M_{xy} \\ M_{yx} + M_{yy} \end{Bmatrix} = \begin{bmatrix} K_{xx}\ K_{xy} \\ K_{yx}\ K_{yy} \end{bmatrix} \begin{Bmatrix} \theta_x \\ \theta_y \end{Bmatrix} \tag{8}$$

where

$$\begin{aligned} K_{xx} &= R^2 \sum_{i=1}^{n} K_{vi} \sin^2(\beta_i), \quad K_{xy} = -R^2 \sum_{i=1}^{n} K_{vi} \sin(\beta_i)\cos(\beta_i) \\ K_{yx} &= R^2 \sum_{i=1}^{n} K_{vi} \sin(\beta_i)\cos(\beta_i), \ K_{yy} = R^2 \sum_{i=1}^{n} K_{vi} \sin^2(\beta_i - \pi/2) \end{aligned} \tag{9}$$

are components of the tilting stiffness.

3.2. Static working point

The dynamic coefficients of the bearings, which must be quantified before dynamic analysis, depend on the static working point of the rotor system. Generally, the static working point could be obtained via the solution of equations including equilibrium equations and deformation-compatibility equations. However, the introduction of thrust bearing makes the problem more complex, especially when the load characteristics are nonlinear. Therefore, the static working point is obtained by numerical simulation based on *ANSYS*.

3.3. Shaft model

3.3.1. Lateral dynamic behavior

In order to predict the effects of the supporting condition of thrust pad on the lateral shaft vibration of hydroelectric generating set, the rotor system is modeled with typical beam finite elements including gyroscopic effects [11,12], as shown in Fig. 4. The governing equations are given as follows

$$[M]\left\{\ddot{U}\right\} + (\Omega[J] + [C])\left\{\dot{U}\right\} + [K]\{U\} = \{F\} \tag{10}$$

where $\{U\} \in R^{4N}$ consists of the generalized displacements including the displacements and deflection angles, N is the total number of the nodes, $[M]$, $[J]$, $[C]$ and $[K]$ are the mass, gyroscopic, damping and stiffness matrixes, respectively. The tilting stiffness caused by the thrust bearing is included in $[K]$. For the guide bearing, the damping is determined in such a way that the vibration amplitudes obtained by numerical simulation are equal to those obtained by test, and the damping of thrust bearing is ignored. $\{F\} \in R^{4N}$ represents the excitation acting on the shaft. The system responses are calculated by the fourth order *Runge-Kutta* method.

3.3.2. Excitation

$\{F\} \in R^{4N}$ consists of the mass unbalance $\{F_{me}\}$, the force caused by misalignment $\{F_{ma}\}$ and unbalance magnetic pull $\{F_{um}\}$.

$$\{F\} = \{F_{me}\} + \{F_{ma}\} + \{F_{um}\} \tag{11}$$

According to the result in [13], the unbalance magnetic pull acting on the generator rotor is represented as

$$\begin{bmatrix} F_{umx} \\ F_{umy} \end{bmatrix} = \frac{R_g L \pi F_j^2}{4\mu_0 r} (2\Lambda_0\Lambda_1 + \Lambda_1\Lambda_2 + \Lambda_2\Lambda_3) \begin{bmatrix} x \\ y \end{bmatrix} \tag{12}$$

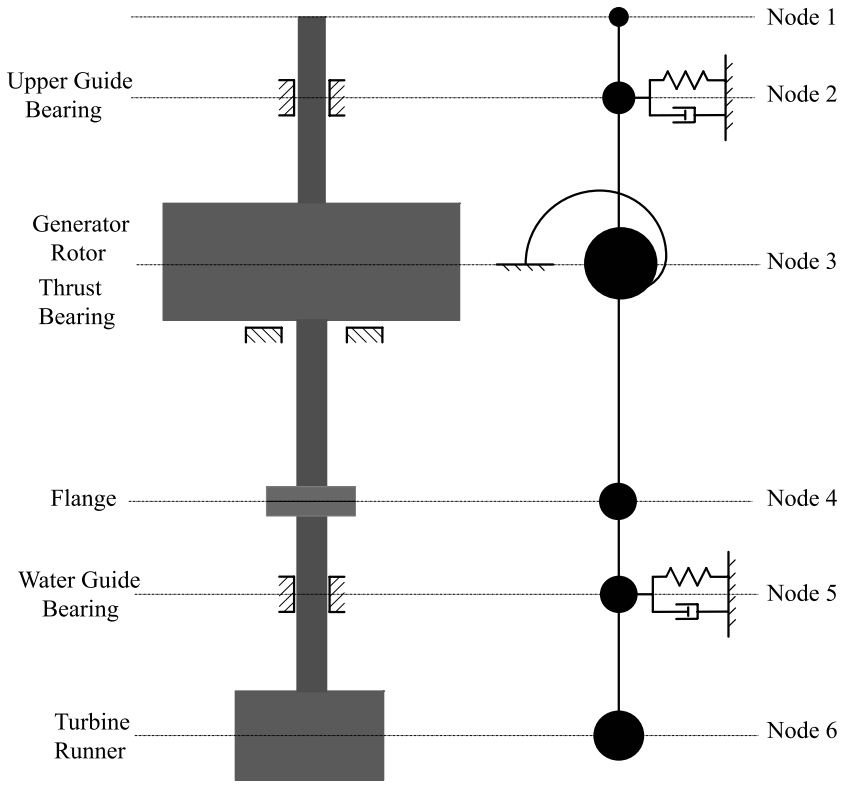

Fig. 4. Schematic diagram of the rotor system.

$$\Lambda_{nu} = \begin{cases} \frac{\mu_0}{\delta_0}\frac{1}{\sqrt{1-\varepsilon^2}} & nu = 0 \\ \frac{2\mu_0}{\delta_0}\frac{1}{\sqrt{1-\varepsilon^2}}\left[\frac{1-\sqrt{1-\varepsilon^2}}{\varepsilon}\right]^{nu} & nu > 0 \end{cases}$$

where μ_0 and δ_0 represent air permeance and mean air-gap length, respectively. $r = (x^2 + y^2)^{1/2}$, $\varepsilon = r/\delta_0$, R_g and L are the radius and height of the generator rotor, and F_j represents amplitude of the fundamental magnetomotive force (MMF) of the excitation current of the generator rotor.

3.4. Load on thrust pad

For hydrodynamic thrust pad, the film thickness decrease with the increment of load. Therefore, when the load on the thrust pad exceeds its limit load, the normal oil film cannot exist between the thrust collar and the thrust pad, and serious faults such as burning tile may occur. As a result, keeping the load on the thrust pad smaller than the limit load is of great importance for the safe and stable operation of the rotor system.

In this paper, the load on thrust pad is divided into two parts which are static load and dynamic load. The static load F_{si} and equivalent axial stiffness K_{vi} of each pad could be obtained in the calculation of static working point, and the dynamic load F_{di} can be calculated from the static characteristic quantity of the single pad as

$$F_{di} = K_{vi} R \left(\theta_y \cos\left(\beta_i\right) - \theta_x \sin\left(\beta_i\right)\right) \tag{13}$$

when the damping of the thrust bearing is ignored. Thus, the load on the ith thrust pad can be obtained as

$$F_i = F_{si} + F_{di}$$

4. Results and discussion

4.1. Parameters

The corresponding parameters of the rotor system are selected according to a real hydroelectric generating set in Fujian province in China: internal radius and external radius of the shaft above the generator $r_u = 0.175$ m, $R_u = 0.330$ m, internal radius and external radius of the shaft under the generator $r_d = 0.275$ m, $R_d = 0.450$ m, the length of first shaft segment which is located between the Node 1 and Node 2 $L_1 = 0.867$ m, the lengths of the other shaft segments $L_2 = 2.124$m, $L_3 = 4.282$ m, $L_4 = 1.95$ m, $L_5 = 1.095$ m, the mass and moment of inertia of generator rotor and turbine runner $m_g = 2.03 \times 10^5$ kg, $I_{pg} = 1.3 \times 10^6$ kgm^2, $I_{dg} = 6.5 \times 10^5$ kgm^2, $m_t = 4.0 \times 10^4$ kg, $I_{pt} = 2.5 \times 10^4$ kgm^2, $I_{dt} = 1.25 \times 10^4$ kgm^2, material density $\rho = 7850$ kg/m^3, material modulus $E = 2.06 \times 10^{11}$ Pa, operational frequency $f = 2.273$ Hz.

The stiffness of the UGB and WGB are $K_{ugb} = 8.82 \times 10^8$ N/m and $K_{wgb} = 1.05 \times 10^9$ N/m, respectively, and the corresponding damping are $C_{ugb} = 9 \times 10^6$ N/m and $C_{wgb} = 1 \times 10^7$ N/m which are determined based on the test data of the hydroelectric generating set. The parameters of the thrust bearing are: external radius and internal radius are $r_1 = 1.15$ m and $r_2 = 0.725$ m, respectively, angular extent of the pad $\theta_0 = 20°$, angular position of the fulcrum $\theta_p = 11.45°$, radius of the circle where the fulcrum is located $R = 0.9475$ m, the dynamic viscosity of oil $\mu = 0.057$ Ns/m^2.

The parameters of the excitation are: eccentric moment of generator rotor, turbine runner and misalignment $me_g = 250$ kgm, $me_t = 50$ kgm, $m\delta_f = 10$ kgm, MMF of excitation current of the generator rotor $F_j = 4200$A.

The limit load of a single pad is set as 6.71×10^5N in accordance with the design criteria.

4.2. Tilting stiffness of thrust bearing

When the elastic oil tanks work normally, the tilting stiffness of thrust bearing is

$$K_{xx} = K_{yy} = 7.22 \times 10^8 Nm$$

However, when the top cover touches the pillar support, the load distribution is variable with the variation of the thrust pad heights. Correspondingly, the axial equivalent stiffness of the thrust pad is also changed due to the nonlinear load characteristics of the oil film. In this case, when all the thrust pads have the same height the tilting stiffness of thrust bearing is

$$K_{xx} = K_{yy} = 3.02 \times 10^{10} Nm$$

Therefore, the tilting stiffness of the thrust bearing increases greatly when the top cover touches the pillar support.

Due to the different operational conditions, the variations of tilting stiffness along with the differences of thrust pad height are calculated, as shown in Figs 5 and 6, where '1, 6 higher' in the legend represents that the 1st and the 6th thrust pads have the same height which is larger than those of other pads.

The results show that the differences of the thrust pad heights have little influence on stiffness coefficients K_{xx} and K_{yy}. On the contrary, the stiffness coefficient K_{xy} varies obviously with the increasing of differences of the thrust pad heights. And all the stiffness coefficients have nearly linear relationship with height difference though the curves are not as smooth as they are supposed to be. The fluctuation is caused by the rounding error and calculation error arising in the data processing and the numerical simulation using *ANSYS*.

Additionally, comparing the curves of '1, 4 high' and '1, 6 high' in Figs 5 and 6, it is easy to find that the distribution of the thrust pad heights has a considerable effect on the stiffness coefficients when the height difference is constant.

It must be pointed out that, the height differences of the thrust pads are selected in a small range here in order to keep the load on thrust pad smaller than the limit load, and the linear relationship may result from the small height difference.

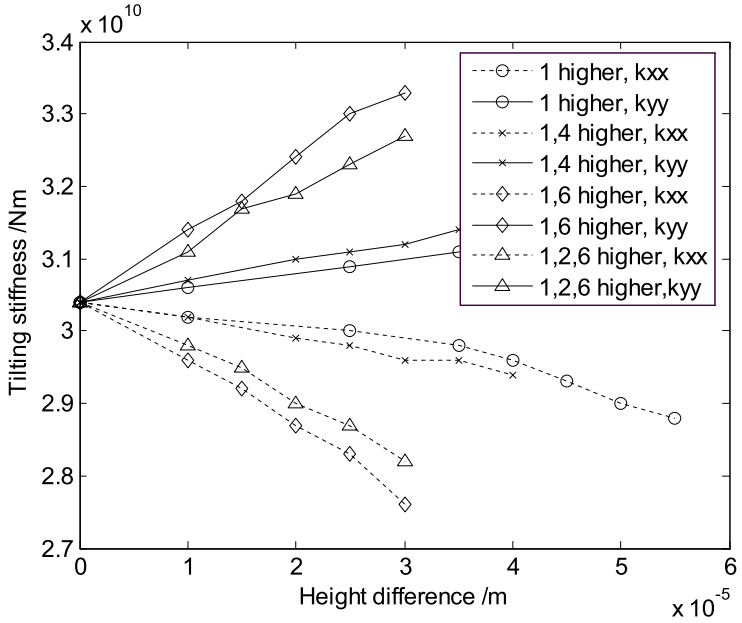

Fig. 5. Stiffness coefficients K_{xx} and K_{yy} versus height difference.

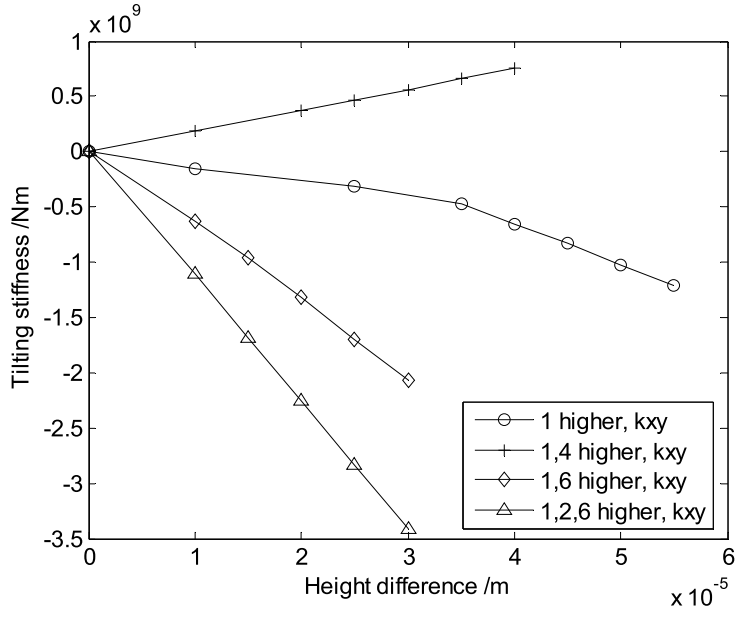

Fig. 6. Stiffness coefficient K_{xy} versus height difference.

4.3. Amplitude of lateral vibration

In order to analyze the influence of the variation of the tilting stiffness of the thrust bearing on the lateral vibration of the hydroelectric generating set, Eq. (10) with different distributions of thrust pad heights is solved, and the results are shown in Fig. 7, where 'without' represents that the influence of the thrust bearing is ignored in the calculation, 'normal' represents that the oil tank works normally, and the case when the oil leakage has happened and all the pads have the same heights is represented by 'abnormal'. From Fig. 7, the following conclusions can be obtained:

Table 1
Effect of thrust bearing on lateral shaft vibration

Node number	1	2	3	4	5	6
A1 (mm)	0.0191	0.0629	0.1961	0.1177	0.0302	0.0208
A2 (mm)	0.0168	0.0640	0.1937	0.1137	0.0290	0.0199
Relative change rate	−11.8%	1.70%	−1.25%	−3.38%	−3.66%	−4.20%

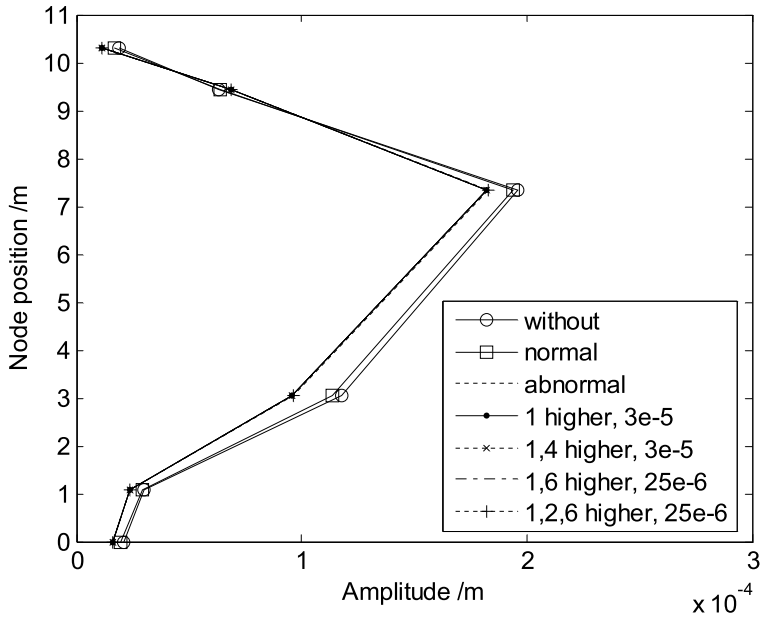

Fig. 7. Amplitudes of lateral shaft vibration with different cases.

– The vibration amplitude of Node 1 and Nodes 3–6 decrease while the amplitude of Node 2 increases after the occurrence of contact between the top cover and the pillar support;
– When the top cover touches the pillar support, the vibration amplitude is small compared with that in the case when the elastic oil tanks work normally;
– The amplitudes are almost the same when the thrust pad heights have different distributions;
– The influence of the thrust bearing on the amplitude of the lateral shaft vibration is small when the elastic oil tanks work normally, as shown in Table 1, where 'A1' and 'A2' represent the amplitude of the lateral shaft vibration when the influence of thrust bearing is ignored and concluded, respectively, and 'Relative change rate' is calculated by (A2-A1)/A1 × 100%.

For the first point, the effect is caused by restraining the tilting movement of the shaft by the thrust bearing. As shown in Fig. 8, the deflection angle in y direction θ_y is negative. When the top cover touches the pillar support, the tilting stiffness of the thrust bearing increases greatly, and the effect could be equivalent to that an additional clockwise moment acts on Node 3. Thus, the amplitude of Node 2 increases while the amplitudes of others are determined by the amplitude changing of Node 2 and the shaft deflection due to the equivalent additional moment. Generally, the amplitude changing of Node 2 is small because of the large stiffness of the guide bearing. Therefore, the variation of the lateral amplitudes of Nodes shown in Fig. 7 is explicable, and the relative change rate displayed in Table 1 could be understood in the same way.

For the second point, the reason is that the action of the thrust bearing is related to the deflection angle where the thrust bearing acts. The larger the deflection angle, the stronger the action. For the rotor system shown in Fig. 4, the deflection angel in Node 3, as shown in Fig. 9, is very small compared with those of other Nodes due to the big moment of inertia and the position in the shaft. Therefore, the effect of the thrust bearing on the lateral vibration of shaft is small. Figure 10 gives the variations of the lateral vibration amplitudes versus the position of

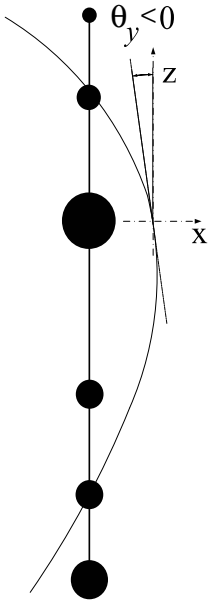

Fig. 8. Deflection angle of Node 3.

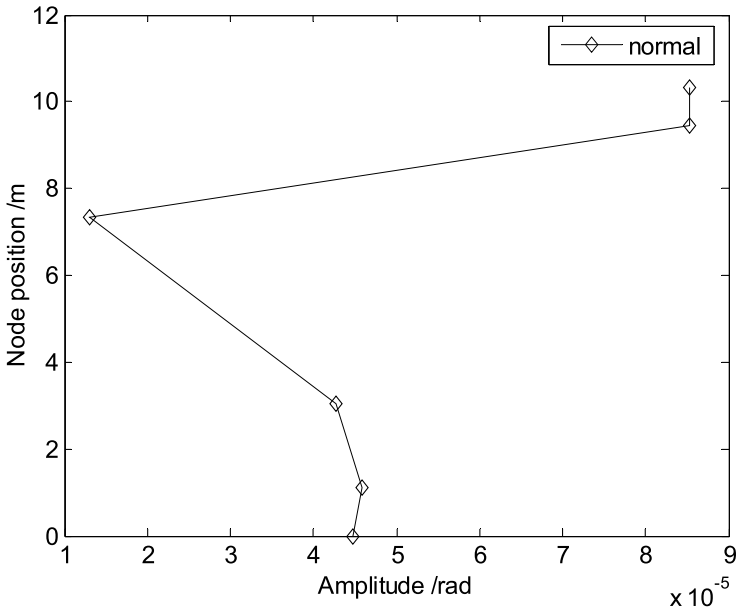

Fig. 9. Deflection angles of shaft when elastic oil tanks work normally.

the thrust bearing, where 'normal-2' represents that elastic oil tank work normally and the thrust bearing is located at Node 2. The results show that for the rotor system shown in Fig. 4, the increasing of tilting stiffness of the thrust bearing makes the amplitudes of Node 3–6 decrease by 5.78%, 15.5%, 16.9% and 18.1%, respectively; however, the corresponding reduce rates are 35.1%, 33.9%, 18.9% and 85.0% respectively when the thrust bearing is located at Node 2.

For the operational conditions shown in Fig. 5, the differences of thrust pad heights have little effect on stiffness coefficients K_{xx} and K_{yy}. Furthermore, the stiffness coefficient K_{xy} is small and the effect is not obvious. Thus,

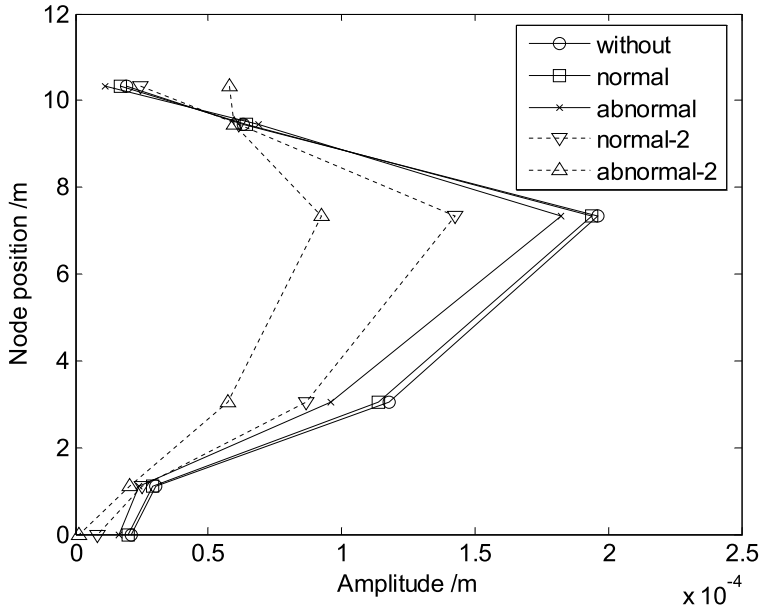

Fig. 10. The influence of the position of the thrust bearing on the lateral vibration.

for the different cases when the top cover touches pillar support, the amplitudes of the lateral shaft vibration are almost the same.

For the last point, the small tilting stiffness due to the connecting oil is another reason besides the small deflection angle at the position where the thrust bearing acts.

4.4. Load on thrust pad

Due to the relative motion of the thrust collar and the differences of thrust pad heights, the load on each thrust pad is investigated, and the maximum load of all pads during the steady state operation of the hydroelectric generating set is shown in Figs 11–13.

Figure 11 shows the case when the height of one pad is larger than those of others. Without loss of generality, the 1st thrust pad is set to be the one with larger height, and it is easy to obtain the conclusion that the maximum load increases with the increasing of the differences of thrust pad heights. Based on the linear hypothesis, the allowable height difference can be calculated according to the limit load of a single pad and the result is 31 μm. When two pads have larger height than those of others, the distribution of the two pads is considered. Figure 12 shows that the allowable high difference decreases with the increasing of dispersion of the two pads which have larger height, and the corresponding allowable high difference are 26 μm, 29 μm, 34 μm, 41 μm, 50 μm. Figure 13 displays the same rule as that shown in Fig. 12, and the smallest allowable high difference is 26 μm which occurs when 1st, 2nd and 6th pads have larger height.

The similar analysis could be performed with other different distributions of the thrust pad heights. The results indicate that the worst case for the hydroelectric generating set displayed in Fig. 4 happens when 1st and 6th have larger height than those of other pads, therefore it is reasonable to draw the conclusion that if the height difference of the thrust pads is less than 26 μm, the load on the thrust pad will not exceed the limit load of a single pad.

5. Conclusions

The tilting stiffness of thrust bearing, vibration amplitude and the load on thrust pad are analyzed to study the lateral vibration of a hydroelectric generating set under various supporting condition of the thrust pad. The results can be summarized as follows:

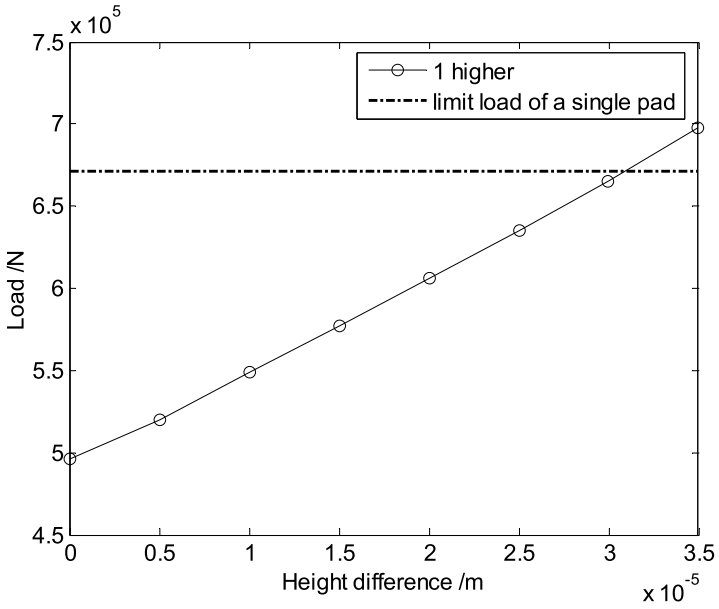

Fig. 11. Maximum load of all pads when one pad has larger height.

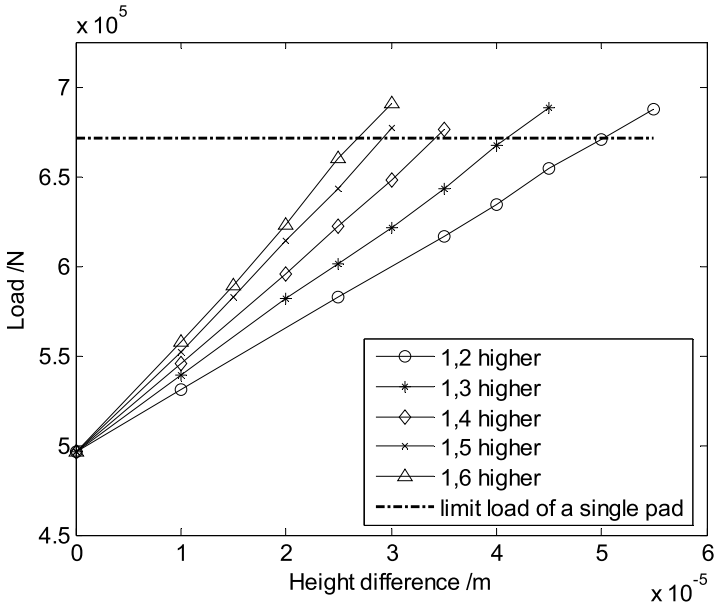

Fig. 12. Maximum load of all pads when two pads have larger heights.

1. The thrust bearing supported by elastic oil tanks has small influence on the lateral shaft vibration when the elastic oil tanks work normally due to the small tilting stiffness.
2. The tilting stiffness of the thrust bearing increases greatly when the top cover touches pillar support.
3. The stiffness coefficients of thrust bearing have linear relationship with the differences of thrust pad height in a certain range while their effect on K_{xy} is more obvious than that on K_{xx} and K_{yy}. And the distribution of the thrust pad heights has considerable effect on the stiffness coefficients.

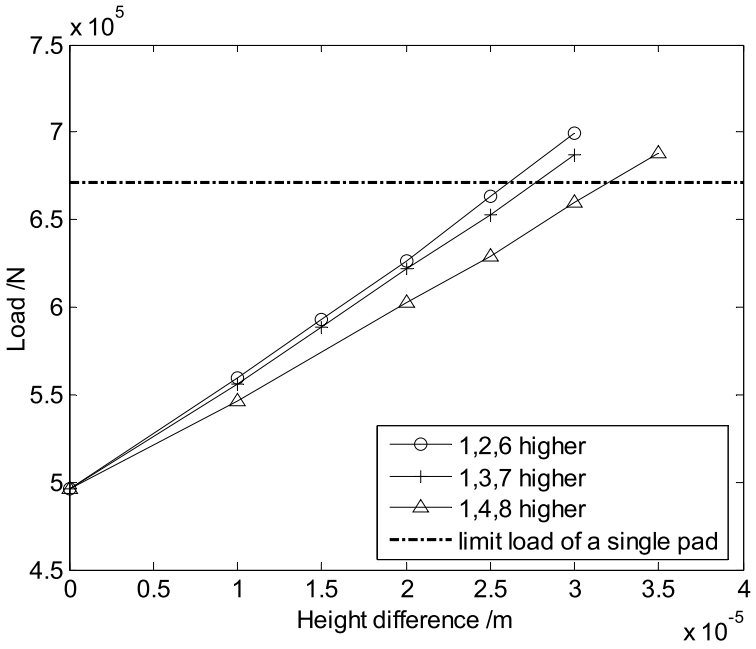

Fig. 13. Maximum load of all pads when three pads have larger heights.

4. The effects of the supporting condition of the thrust pads on the amplitude of the lateral shaft vibration is not obvious because the thrust bearing is placed in the position where its action is not strong and the stiffness coefficients do not vary greatly.
5. The difference of thrust pad heights is of great importance for the load on the thrust pad, and the height difference of any two thrust pads should not exceed 26 μm in order to guarantee the safe and stable operation of the hydroelectric generating set.

Since the influence of the thrust bearing on the lateral shaft vibration can be affected by many factors, such as axial load, stiffness of the shaft, static load on the journal bearings, position and arrangement of the thrust bearing et al, more analyses are required to draw the more general conclusions. Besides, the dynamic response is calculated based on the linear hypothesis and only the main supporting conditions are considered in this paper. Therefore, more accurate result will be obtained when more precise models are introduced.

Acknowledgments

This research is supported financially by National Science Foundation of China (Grant No. 10702031, 10732060).

References

[1] T. Someya and M. Fukuda, Analysis and Experimental Verification of Dynamic Characteristics of Oil Film Thrust Bearings, *Bulletin of JSME* **15** (1972), 1004–1015.
[2] E. Storteig and M.F. White, Dynamic Characteristics of Hydro-Dynamically Lubricated Fixed-Pad Thrust Bearing, *Wear* **232** (1999), 250–255.
[3] Q. Zhu, Y.B. Xie and L. Yu, Axial Transient Forces of Thrust Bearing Rotor System in a Turboexpander, *Proceedings of International Conference on Hydrodynamic Bearing-Rotor System Dynamics*, Xi'an, China, 1990.
[4] P.L. Jiang and L. Yu, Identification of the Oil-Film Dynamic Coefficients in a Rotor-Bearing system with a Hydrodynamic Thrust Bearing, *Journal of Sound and Vibration* **236** (2000), 733–740.
[5] T.W. Dimond, P.N. Sheth, P.E. Allaire and M. He, Identification methods and test results for tilting pad and fixed geometry journal bearing dynamic coefficients – A review, *Shock and vibration* **16** (2009), 13–43.

[6] N. Mittwollen, T. Hegel and J. Glienicke, Effect of Hydrodynamic Thrust Bearings on Lateral shaft vibrations, Transactions of ASME, *Journal of Tribology* **113** (1991), 811–818.
[7] L. Yu and R.B. Bhat, Coupled dynamics of a Rotor-Journal Bearing System Equipped with Thrust Bearings, *Shock and Vibration* **2** (1995), 1–14.
[8] P.L. Jiang and L. Yu, Effect of a Hydrodynamic Thrust Bearing on the Statics and Dynamics of a Rotor-Bearing System, *Mechanics Research Communications* **25** (1998), 219–224.
[9] P.L. Jiang and L. Yu, Dynamics of a rotor-bearing system equipped with a hydrodynamic thrust bearing, *Journal of Sound and Vibration* **227** (1999), 833–872.
[10] S. Berger, O. Bonneau and J. Frêne, Influence of Axial Thrust Bearing on the Dynamic Behavior of an Elastic Shaft: Coupling Between the Axial Dynamic Behavior and the Bending Vibration of a Flexible Shaft, *Journal of Vibration and Acoustics* **123** (2001), 145–149.
[11] H.D. Nelson, A Finite Rotating Shaft Node using Timoshenko Beam Theory, Transactions of ASME, *Journal of Mechanical Design* **102** (1980), 793–803.
[12] H. Nevzat özgüven and Z. Levent özkan, Whirl Speeds and Unbalance Response of Multibearing Rotors using Finite Node, Transactions of ASME, *Journal of Vibration, Acoustics, Stress, and Reliability in Design* **106** (1984), 72–79.
[13] D. Guo, F. Chu and D. Chen, The Unbalanced Magnetic Pull and its Effects on Vibration in a Three-Phase Generator with Eccentric Rotor, *Journal of Sound and Vibration* **54** (2002), 297–312.